Astron. Astrophys. 357, 1105–1114 (2000)

ASTRONOMY AND ASTROPHYSICS

Temporal dynamics of Joule heating and DC-electric field acceleration in single flare loop

V.V. Zaitsev[1], **S. Urpo**[2], **and A.V. Stepanov**[3]

[1] Institute of Applied Physics, Ulyanova 46, N. Novgorod 603600, Russia
[2] Metsähovi Radio Observatory, Metsähovintie 114, 02540 Kylmälä, Finland
[3] Central Astronomical Observatory at Pulkovo, St. Petersburg 196140, Russia

Received 7 February 2000 / Accepted 14 March 2000

Abstract. Pulsating and explosive time profiles of mm-wave solar bursts observed at Metsähovi are examined in terms of the energy release in a single current-carrying loop. We suppose that the electric current in the loop is driven by photospheric convective flows. The flare occurs due to flute instability provoking the penetration of partially ionized plasma from the chromosphere or prominence into the current channel of a loop and increasing the loop resistance by many orders of magnitude. The feedback of deviation of the loop magnetic field on the energy release rate is taken into account. Joule plasma heating due to current dissipation and electron acceleration in DC electric field are considered. Both processes act simultaneously and are driven by one parameter, the penetration depth of partially ionized plasma into the current-carrying loop. Two regimes of energy release are studied: (i) Pulsating energy release in current-carrying loops with negative radial gradient of gas pressure; (ii) Explosive plus pulsating energy release in a loop with positive radial gradient of gas pressure. One can explain the various time behaviours of the flares, for example, several quasi-periodic pulses, and pulsations with increasing amplitude at pre-flash phase followed by explosive enhancement of the emission at flash phase. The possibility of powerful flare in current-carrying magnetic loop with plasma beta $\beta \ll 1$ is discussed.

Key words: acceleration of particles – plasmas – Sun: activity – Sun: chromosphere – Sun: flares – Sun: radio radiation

1. Introduction

Radio and hard X-ray observations of solar flares provide evidence of pulsations in the flare emission. Some events show several quasi-periodic pulses during the flare (Kane et al. 1983; Nakajima et al. 1983). Other events start with several pulses with enhanced amplitude in the pre-flash phase which exhibit then an explosive energy release (flash phase) (Benz et al. 1983; Urpo et al. 1992; Lee & Wang 1998). Both pre-flash and flash phases make up the impulsive phase (Benz et al. 1983). After the flux maximum, the long-term modulation has lower amplitude (a few percent) and persists often throughout the entire gradual decay phase of the flare (Urpo et al. 1992). Long-term modulation was interpreted in the frame of equivalent LRC-circuit oscillations (Zaitsev et al. 1998).

A number of papers are devoted to the origin of pulse structures in solar flare emission. Sakai & de Jager (1996) reviewed the flare pulsations and their fine structure and explained them in terms of collisions between current-carrying loops (see also Tajima et al. 1987; Chargeishvili et al. 1993; Nishikawa et al. 1994; Sakai & de Jager 1997). Two-current-loop coalescence can explain quasi-periodic amplitude oscillations and double sub-peak structure. Sakai & de Jager (1996) mentioned that "flares are different". A two-loop interaction model cannot explain various time histories of the flare energy release. In particular single-loop flares are also possible. Indeed, X-ray and microwave image data from Skylab, SMM, Yohkoh, VLA, Nobeyama, and TRACE suggest that in many cases the flare occurs in a single loop (Marsh & Hurford 1980; Masuda 1994; Doshek et al. 1995; Sakao & Kosugi 1996; Enome 1996; Kucera et al. 1996; Sato et al. 1998; Ciuderi Drago et al. 1998; Schrijver et al. 1999). Also the emission from simple flare loop shows pulsations. Fig. 1 presents two examples of such events in the hard (14–53 keV) X-ray emission (Sato et al. 1998). Alfvén & Carlqvist (1967), Heyvaerts et al. (1977), Spicer (1977), Colgate (1978), Uchida & Shibata (1988), Zaitsev & Stepanov (1992), Tsuneta (1996), Zaitsev & Khodachenko (1997) considered the flare energy release in the frame of a simple loop approach. To interpret the pulses, MHD-oscillations of a magnetic loop have been used (Rosenberg 1970; Roberts et al. 1984; Aschwanden 1987; Stepanov et al. 1992). Gas pressure in the coronal part of the loop can rise fast due to prompt energy release. As a consequence, the radial fast magneto-sonic oscillations of a magnetic arch appear. Alfvén-type oscillations of a magnetic loop can arise during the evaporation of chromosphere plasma (Stepanov et al. 1992) or in response of a loop to the injection of magnetic flux (Cargill et al. 1994). Recently we proposed a model of long-term pulsations of mm-wave emission arising due to electric current oscillations in a magnetic loop as an equivalent LRC-circuit (Zaitsev et al. 1998). Using this model the electric currents in flare loops were estimated to as high as 6×10^{10} - 1.4×10^{12} A.

Send offprint requests to: A.V. Stepanov (stepanov@gao.spb.ru)

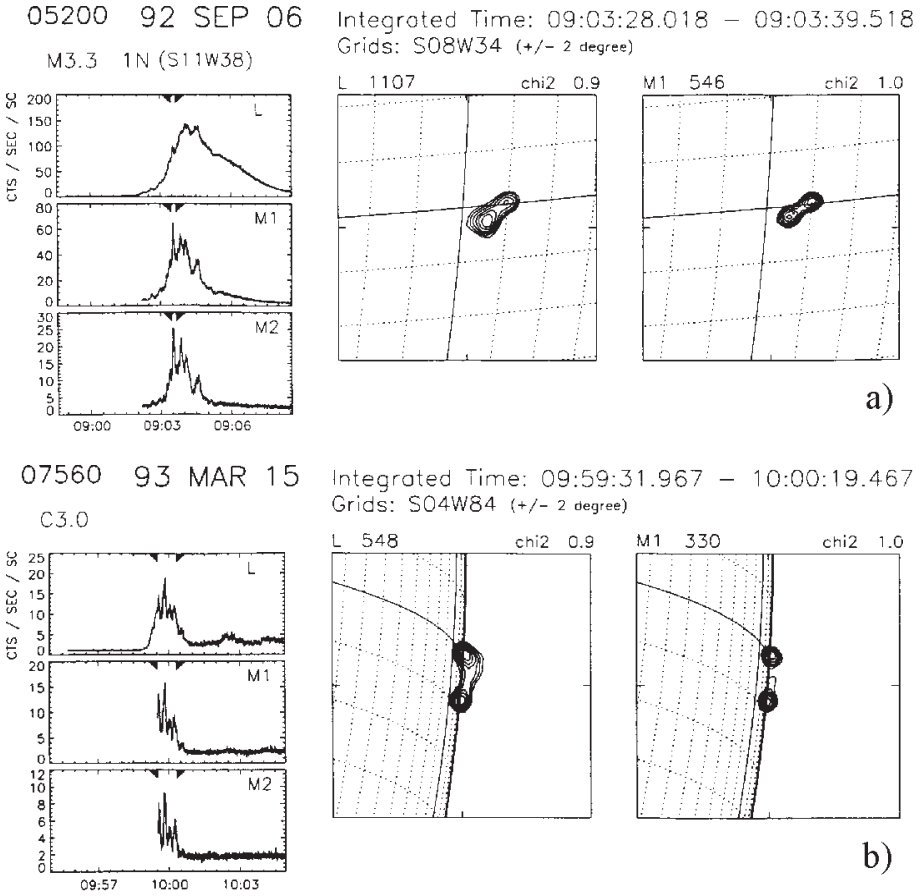

Fig. 1a and b. Two examples of simple loop flares in 14–53 keV emission observed by Yohkoh (Sato et al. 1998). **a** 1992 September 6, 0903 UT, **b** 1993 March 15, 0959 UT

In pulsation models, the non-self-consistent approach has been applied because only the influence of the variation of the loop magnetic field on the modulation of radio and X-ray emission was considered. Moreover, most of the above mentioned models do not explain the explosive energy release.

In this paper we consider the temporal dynamics of Joule heating of plasma and DC-electric field acceleration of electrons in a single current-carrying loop and interpret both the pulsating and the explosive energy releases in the impulsive phase of a flare. As an example we consider an advanced circuit model (Zaitsev & Stepanov 1992; Zaitsev et al. 1998) based on the idea of Alfvén & Carlqvist (1967) where the solar flare is described as an equivalent electric circuit. According to this model the flare energy release occurs in a current-carrying coronal magnetic loop due to the injection of partially ionized plasma into the current channel from the prominence (near the loop top) or from the chromosphere (at the loop foot-points). This process is driven by the flute instability. The loop conductivity drops by many orders of magnitude due to ion-atom collisions (Cowling conductivity). As a result the effective current dissipation leads to a flare. We propose a self-consistent model in which the feedback of the magnetic field variations is taken into account on the penetrating "tongue". This allows us to consider both the pulsating and explosive regimes of the energy release in the temporal dynamics of solar flares. We avoid the difficulties of the energy release mechanism in a current-carrying loop with plasma beta $\beta \ll 1$, which was mentioned by Wheatland & Melrose (1995). Both plasma heating and particle acceleration are driven by one parameter, the penetration depth of a plasma "tongue" into the current-carrying loop.

In Sect. 2 we describe Metsähovi mm-wave observations of flares. A self-consistent approach for Joule heating and DC-particle acceleration in single current loops is considered in Sect. 3. Solutions for pulsating and explosive energy release are given in Sect. 4. The results are discussed in Sect. 5.

2. Observations

We report on selected solar flares observed in Metsähovi at 22 and 37 GHz (Urpo et al. 1992). These examples reveal various time behaviour of the flares. In accordance with our approach we divide the time profiles into three groups.

(i) Set of pulses. Fig. 2a shows the burst of 1991 June 11, 0915 UT revealing pulses with growing and then decreasing amplitude. The modulation magnitude was not so large as compared to the event of 1991 March 22, 0903 UT (Fig. 2b). The event in Fig. 2b consists of three peaks and quite similar to that observed by Kane et al. (1983). From the analysis of Metsähovi data at 22 and 37 GHz we found a lot of such a type of events having 3–6 pulses with time scales of 3–80 s, and with maximum flux between 7 and 100 sfu.

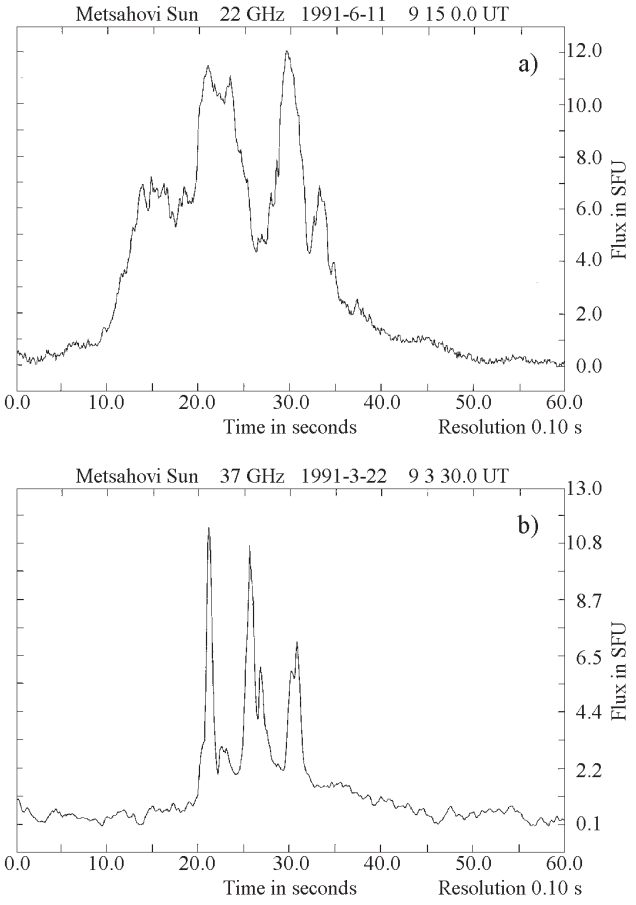

Fig. 2a and b. The time profiles of mm-wave emission consisting from several pulses. **a** 1991 June 11, 0915 UT (22 GHz), **b** 1991 March 22, 0903 UT (37 GHz)

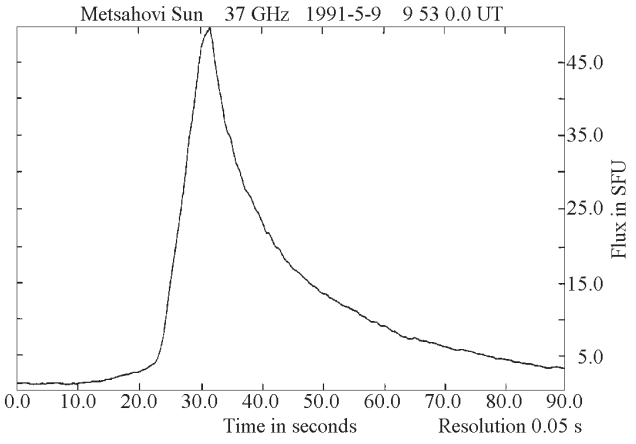

Fig. 3. Example of flare emission at 37 GHz with time resolution 0.05 s in the form of single pulse (event of May 9, 1991, 0953 UT)

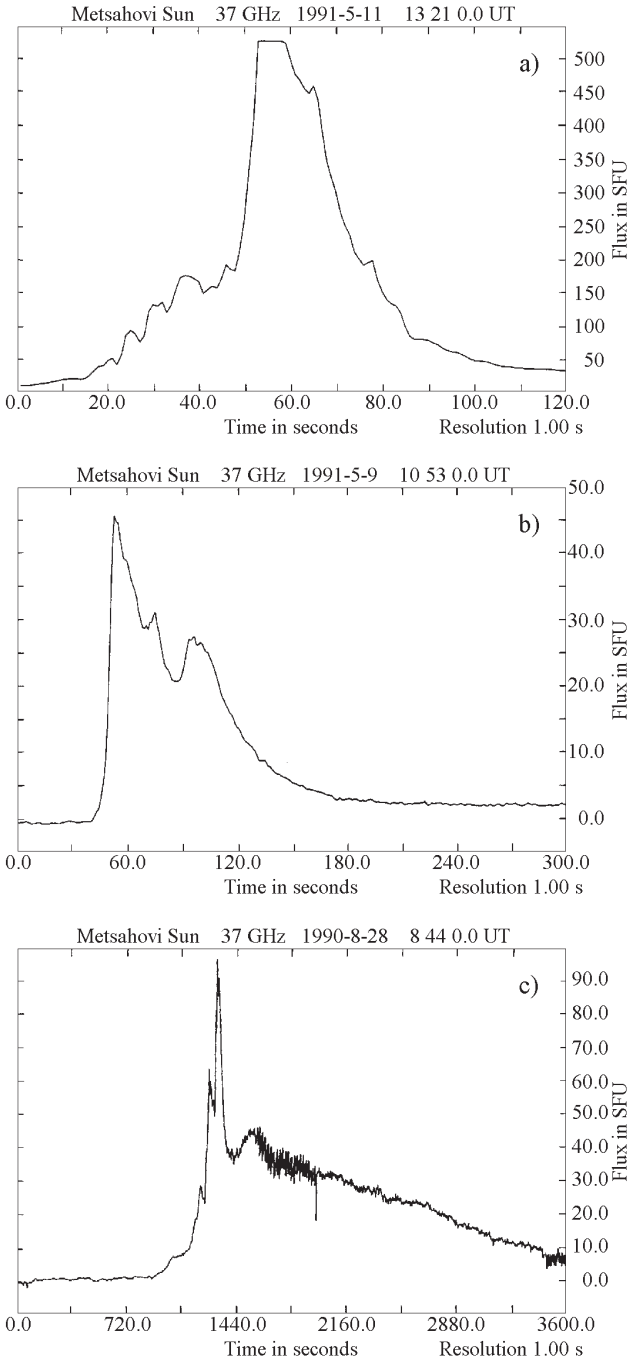

Fig. 4. a The time profile of 37 GHz emission on 1991 May 11, 1321 UT with enhanced pulses at pre-flash phase followed by the explosive phase. **b** The event of May 9, 1991, 1053 UT with explosive rise phase followed. by pulses. **c** The event of August 28, 1990, 0846 UT with pulses superimposed upon explosive profile.

(ii) Single pulse events. Fig. 3 presents an example of a single pulse event of May 9, 1991 0953 UT. The flux of mm-wave emission grows up to 50 sfu during a few seconds and than shows an e-folding decay with time scales of about ten seconds. It is important to note that no fine structure was observed at least within the time resolution of 0.05 s. Several events of the same character with maximum flux of 8–50 sfu and decay time 0.5–3 min were observed also at 22 and 37 GHz.

(iii) Pulses before, after, and during the explosive phase. Time profile of the 37 GHz emission of the event of May 11, 1991 is shown in Fig. 4a (Urpo et al. 1992). The burst starts with six ~ 10 s pulses of enhanced amplitude at pre-flash phase and then evolves into explosive (non-exponential) energy release. The

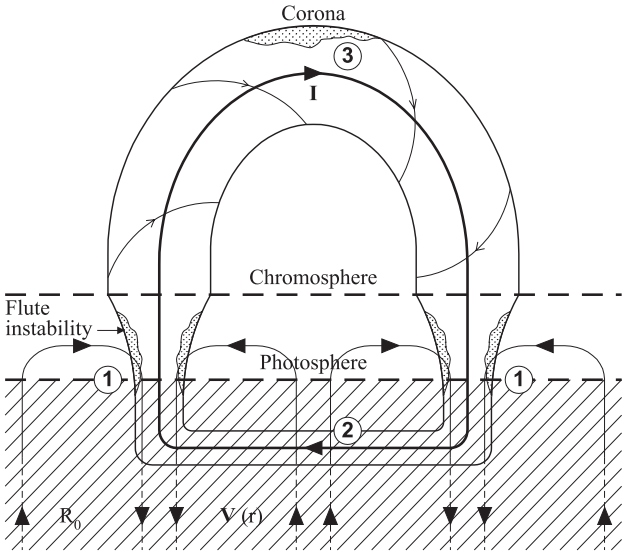

Fig. 5. Cartoon model of current-carrying magnetic loop. Converging convective plasma flows generate the electric current in region 1. This current flows trough coronal part of a loop from one foot-point to another and closes just under photosphere (slightly below the level of $\tau_{5000} \approx 1$) where conductivity becomes isotropic (region 2). In region 1 located between chromosphere and photosphere the flute instability arises. The resistance of current channel in region 1 grows by many orders due to flute instability and it leads to the flare. The same situation can be realized also near the loop top due to the loop-prominence interaction (region 3)

emission flux reaches its maximum value of about 530 sfu four seconds later. After maximum a long-term decay lasts for about 40 min. This event is very similar to the flare of 2 November 1991, reported by Lee & Wang (1998) with one difference: the time scale of pulsations in the event of 2 November 1991 at pre-flash phase is about two minutes (about one order of magnitude longer). Fig. 4b presents the explosive rise phase followed by pulsations in the event of May 9, 1991 1053 UT. The pulsation time scale varies from 15 to 30 s. It is seen from Fig. 4c that both pulsation and explosive phases co-exist simultaneously.

Unfortunately, we have no direct evidence for a simple loop origin of the events presented in Figs. 2–5 because no microwave and X-ray maps with high spatial resolution were available for these events. Nevertheless, except for numerous evidences of simple loop flares (see, for example, the review by Sakai & de Jager (1996) and Fig. 1) there is an additional indirect argument in favor of a single loop origin. The bursts under consideration (except the event of May 11, 1991) have comparatively short duration and are rather weak, < 100 sfu as it should be for simple-loop compact flares (Priest 1985). Two-loop and multi-loop flares produce more powerful radio emission.

3. Single-loop flare model

Single-loop flare (or compact flare) models are described in detail in several reviews (e.g. Priest 1985; Sakai & de Jager 1996). These models can be divided into two classes: (1) magnetic reconnection models and (2) electric current dissipation models. To the first class belongs the model of Heyvaerts et al. (1977), in which the loop-like emerging flux reconnects with the overlaying magnetic field. Spicer's (1977) model suggests that twisting magnetic field lines of a coronal arch leads to the tearing instability which is responsible for the conversion of the magnetic field energy into plasma heating and particle acceleration. However the resistive tearing-mode instability is too slow to explain the impulsive phase of a flare. Sakai & de Jager (1996) proposed that the flare may either by due to fluxthread interaction, or else be provoked by forces from outside such as emerging flux. Yohkoh observations induced single-loop cusp-type model described by Tsuneta et al.(1992) and Masuda (1994). One serious problem with the cusp-type model is that the magnetic field is too low (20–30 G) in reconnection region to explain the observed flare power. A magnetodynamic flare mechanism based on the interaction of two sweeping pinches at the top of a symmetric loop leading to the annihilation of the magnetic energy has been proposed by Uchida & Shibata (1988).

The Alfvén-Carlqvist flare model is based on the dissipation of electric current in a coronal loop, which forms an equivalent electric circuit. The current is generated by photospheric convection, and the sudden increase of the loop resistance (current interruption) is due to formation of electric double layers. In the phenomenological model of Colgate (1978) the flare occurs due to dissipation of the azimuthal magnetic field B_φ that is induced by the electric current along the loop. Zaitsev & Stepanov (1992) suggested that the partially ionized plasma and non-steady-state conditions play a decisive role in the flare energy release. Partially ionized plasma can penetrate into the loop current channel from the prominence located near the loop top (Pustil'nik 1973; Zaitsev & Stepanov 1992) or otherwise from the chromosphere (Zaitsev & Khodachenko 1997). In both cases the flare trigger is the flute instability.

3.1. Current-carrying steady-state loop

In studying the reasons for various kinds of the temporal dynamics of flare emission during impulsive phase we consider a coronal magnetic loop with footpoints embedded into the photosphere and formed by the converging flow of photospheric plasma. This structure can be formed when the loop footpoints are located in the nodes of supergranulation cells (Bray et al. 1984). The equivalent electric circuit consists of three domains (Fig. 5). The magnetic field and the associated electric currents are generated in region 1 located in the photosphere and lower chromosphere. In this region the electrons are more closely bound to the magnetic field lines than the positive ions. Consequently, the neutrals hydrogen atoms in the convective flow are better able to carry the ions. A radial electric field E_r develops due to charge separation. Together with the initial magnetic field B_z it generates a Hall current j_φ and strengthens B_z (Sen & White 1972). In this region the electro-motive force $(e.m.f.)$ driven by the photospheric convection (Zaitsev et al. 1998) is

$$e.m.f. = \frac{H}{\pi r_0^2 c} \int_0^{r_0} V_c B_\varphi 2\pi r \, dr \, .$$

with H the thickness of region 1, r_o the flux tube radius, B_φ the azimuthal magnetic field, $V_c \approx 0.3$–1 km s^{-1} the horizontal velocity of convective flow (Bray et al. 1984). This $e.m.f.$ supports the electric current in the flux tube, which flows from one footpoint to the other and closes in the photosphere (region 2) at the level where the conductivity becomes isotropic, corresponding to the level $\tau_{5000} = 1$. Region 3 is the coronal part of the loop. Here plasma beta $\beta \ll 1$, and the loop magnetic field is force-free, i.e. the electric currents flow along magnetic field lines.

The amplification of the loop magnetic field due to the generation of Hall currents j_φ continues until the field enhancement caused by the converging convective flow is compensated by the magnetic field diffusion due to finite plasma conductivity in region 1. A steady-state magnetic loop is formed. The loop magnetic field is determined by the total energy input of the convective flow during the time of loop formation (of the order of R_0/V_c, R_0 is the scale of supergranulation cell). The electric current value in a flare magnetic loop is of the order of $10^{11} - 10^{12}$ A (Zaitsev et al. 1998). For the energy release rate in a solar flare $RI^2 \sim 10^{20}$ W with this currents one needs a resistance $R \sim 10^{-4} - 10^{-2}$ Ohm. Classical Spitzer resistivity gives $R \sim 10^{-11}$ Ohm in the solar corona and photosphere (Kan et al. 1983; Zaitsev & Stepanov 1992). Hence, for the solar flare the resistance should increase by 7–9 orders of magnitude.

3.2. Joule heating

What is the origin of the flare energy release in single current-carrying coronal loops? One of the possible triggers of the flare is the flute instability (Pustil'nik 1973; Zaitsev & Stepanov 1992; Zaitsev & Khodachenko 1997). Penetration of partially ionized plasma from the prominence or the surrounding chromosphere into the current channel of a loop gives a very effective electric current dissipation caused by ion-atom collisions. In this case the rate of Joule heating can be described by the generalized Ohm's law (see e.g. Cowling 1957)

$$\mathbf{E} + \frac{1}{c}\mathbf{V}\times\mathbf{B} = \frac{\mathbf{j}}{\sigma} + \frac{\mathbf{j}\times\mathbf{B}}{en_e c} - \frac{\nabla p_e}{en_e} \\ \frac{F}{cn_e m_i \nu_{ia}}(\nabla p_a \times \mathbf{B} + F\rho\frac{d\mathbf{V}}{dt}\times\mathbf{B}) \quad (1)$$

Here p_a and p_e are the neutral gas and electron pressures, respectively, $\sigma = e^2 n_e/m_e(\nu_{ei} + \nu_{ea})$ is the Coulomb conductivity, ν_{ei}, ν_{ea} and ν_{ia} are electron-ion, electron-atom and ion-atom collision frequencies, respectively, $\mathbf{V} = \sum\limits_k n_k m_k \mathbf{V}_k / \sum\limits_k n_k m_n$ is the velocity of bulk plasma ($k = a, i, e$), which is determined from the motion equation

$$\rho\frac{d\mathbf{V}}{dt} = \frac{1}{c}\mathbf{j}\times\mathbf{B} - \nabla p \quad (2)$$

with $p = p_a + p_i + p_e$ and $\rho = n_a m_a + n_i m_i + n_e m_e$ being the total gas pressure and the total plasma density, respectively, $F = n_a m_a/(n_a m_a + n_i m_i + n_e m_e)$ is the relative density of neutrals. In the case $\frac{1}{c}|\mathbf{j}\times\mathbf{B}| \gg |\nabla p|$ we obtain from Eqs. (1) and (2) the formula for the rate of Joule dissipation:

$$q = (\mathbf{E} + \frac{1}{c}\mathbf{V}\times\mathbf{B})\mathbf{j} = \frac{F^2}{c^2 n m_i \nu_{ia}}(\mathbf{j}\times\mathbf{B})^2 \quad (3)$$

Here and below we use the definition $n \equiv n_e = n_i$. In steady state the current-carrying coronal magnetic loop is force-free. Here the gas pressure inside the loop is much less than the magnetic field pressure, $\beta = 8\pi p/B^2 \ll 1$. Thus, the electric current $\mathbf{j}$ is approximately parallel to the magnetic field $\mathbf{B}$ ($\mathbf{j} \parallel \mathbf{B}$), and the energy release is very small. When a "tongue" of surrounding chromosphere plasma penetrates into the current channel of the loop due to the flute instability, the loop magnetic field is deformed in accord with the equation

$$\frac{\partial\mathbf{B}}{\partial t} = \nabla\times\left[(\mathbf{V} + \frac{F^2\rho}{nm_i\nu_{ia}}\frac{d\mathbf{V}}{dt})\times\mathbf{B}\right] \quad (4)$$

As a result the loop resistance can be as high as $R \approx 4I^2HF^2/(c^4 n m_i \nu_{ia}\pi r_0^4) \approx 10^{-3}$ Ohm (Zaitsev et al. 1998).

The threshold of the ballooning mode of the flute instability (Mikhailovskii 1975) can be represented as $\beta > 2\pi H r_0/L^2$, where H is approximately equal to the scale of the transition region between the photosphere and the chromosphere (L is the loop length). For $H \sim$ 400–500 km, $r_0 \sim 10^3$ km and $L \sim 10^4$ km which gives $\beta > 0.03$. The plasma beta in the chromosphere can be estimated as $\beta \sim 0.01$, hence the flute instability threshold can be easily reached due to, for instance, local heating or plasma compression. We suppose the following approximation for the radial component of the velocity field of the tongue (Henoux & Somov 1991): $V_r(r,t) = V_0(t)r/r_0$, $r \le r_0$. In such a case, both B_z and B_φ inside the flux tube, can be represented as (Zaitsev & Khodachenko 1997):

$$B_\varphi(r,t) = e^y B_{\varphi_0}(re^y),\ B_z(r,t) = e^y B_{z_0}(re^y), \\ y = -\frac{1}{r_0}\int\limits_0^t\left(V_0(t') + \frac{F^2\rho}{nm_i\nu_{ia}}\frac{dV_0}{dt'}\right)dt' \quad (5)$$

If the initial magnetic flux tube is force-free ($\mathbf{j}\times\mathbf{B} = 0$), for example (Priest 1982)

$$B_{\varphi_0} = \frac{r}{r_0}\frac{B_0}{1 + r^2/r_0^2},\ B_{z_0} = \frac{B_0}{1 + r^2/r_0^2} \quad (6)$$

the force-free field is disturbed by the flute instability according to Eq. (5). Ampère's force becomes

$$\frac{1}{c}\mathbf{j}\times\mathbf{B} = \frac{B_0^2\mathbf{r}}{2\pi r_0^2}\frac{e^{4y}(e^{2y}-1)}{(1 + \frac{r^2}{r_0^2}e^{2y})^3} \quad (7)$$

This force for $V_0(0) < 0$, pushes the penetrating plasma out of the current channel. At the same time it follows from Eq. (3) that the Ampère force produces strong Joule heating inside the current loop. The variation of the gas pressure in the loop is described by

$$\frac{1}{\gamma - 1}\frac{dp}{dt} = \frac{F^2 B_0^4}{nm_i\nu_{ia}}\frac{r^2}{4\pi^2 r_0^4}\frac{e^{8y}(e^{2y}-1)^2}{(1 + \frac{r^2}{r_0^2}e^{2y})^6} \quad (8)$$

where $\gamma = c_p/c_v$ is the ratio of specific heats. Hence we obtain the self-consistent set of equations for the plasma velocity and gas pressure. It provides information about the time evolution of the energy release in the impulsive phase of the flare.

Consider now the case, when the velocity of penetrating plasma is small compared to the Alfvén velocity ($|V_0| \ll V_A$). We investigate the region of the flux tube near its axis ($r^2 \ll r_0^2$). The distribution of the gas pressure can be approximated by

$$p(r,t) = p_{0_0}(t) + p_0(t)\frac{r^2}{r_0^2} \tag{9}$$

We can use also $\partial/\partial t$ instead of $d/dt = \partial/\partial t + \mathbf{V}\partial/\partial \mathbf{r}$, because the velocity of the penetrating plasma is small. As a result, we obtain the following set of equations

$$e^{2y}\rho_0\frac{\partial V_0}{\partial t} = -\frac{2p_0}{r_0} + \frac{B_0^2}{2\pi r_0}e^{4y}(e^{2y}-1) \tag{10}$$

$$\frac{\partial p_0}{\partial t} = \frac{(\gamma-1)F^2B_0^4}{nm_i\nu_{ia}4\pi^2r_0^2}e^{8y}(e^{2y}-1)^2 \tag{11}$$

$$y = -\frac{1}{r_0}\int_0^t \left(V_0(t') + \frac{F^2\rho}{nm_i\nu_{ia}}\frac{dV_0}{dt'}\right)dt' \tag{12}$$

We will use the approximation $y \ll 1$ which means that the oscillation amplitude of a tongue is much less than the loop radius. With this assumption Eqs. (10)-(12) read

$$\frac{\partial V_0}{\partial t} = -\frac{2p_0}{r_0} + \frac{B_0^2}{\pi r_0}y \tag{13}$$

$$\frac{\partial p_0}{\partial t} = \frac{(\gamma-1)F^2B_0^4}{nm_i\nu_{ia}\pi^2r_0^2}y^2 \tag{14}$$

$$\frac{\partial y}{\partial t} = -\frac{V_0}{r_0} - \frac{F^2\rho}{nm_i\nu_{ia}r_0}\frac{\partial V_0}{\partial t} \tag{15}$$

Combining Eqs. (13)-(15) yields

$$\frac{\partial^3 y}{\partial\tau^3} + \varepsilon_1\frac{\partial^2 y}{\partial\tau^2} + \frac{\partial y}{\partial\tau} - 2\varepsilon\varepsilon_1 y\frac{\partial y}{\partial\tau} = \varepsilon y^2 \tag{16}$$

Here we introduced the following definitions:

$$t_c = 2(\gamma-1)F^2\frac{n+n_a}{n}\frac{1}{\nu_{ia}},\ t_A = \frac{r_0}{2V_A},\ \tau = \frac{t}{t_A}$$
$$V_A = \frac{B_0}{\sqrt{4\pi\rho_0}},\ \varepsilon = \frac{t_c}{t_A},\ \varepsilon_1 = \frac{\varepsilon}{2(\gamma-1)} \tag{17}$$

The ratio $\varepsilon = t_c/t_A$ is the parameter of the effectiveness of Joule heating of the plasma. It varies in a wide interval depending on the magnetic field value, the tube radius as well as number density, temperature, and ionization ratio of the plasma which penetrates into the loop due to the flute instability. ε_1 describes the efficiency of dissipation of MHD-oscillations of the current channel by ion-atom collisions. From Eq. (14) it follows that temporal dynamics of plasma Joule heating depends on the function $y(t)$ which, in turn, determines from Eq. (16).

3.3. Particle acceleration

The time-dependence of $y(t)$ also determines the temporal dynamics of charged particle acceleration by the large-scale electric fields in a simple magnetic loop. The electric field of the current in a plasma with classical and/or anomalous conductivity (see e.g. Holman 1985; Tsuneta 1985) is small. In order to supply sufficiently high current densities very thin current sheets are required. Here we consider electron acceleration by the electric fields driven by charge separation which arises in a current-carrying flux tube. Such charge separation electric fields are larger than the electric fields from plasma conductivity.

It is well known that in the case of $|\mathbf{E}| < |\mathbf{B}|$ only the electric field directed along the magnetic field takes part in electron acceleration. From the generalized Ohm's law (Eq. 1) one can find the electric field component parallel to the magnetic field:

$$E_\parallel = \frac{\mathbf{EB}}{B} = \frac{j_\parallel}{\sigma} - \frac{\nabla p_e \mathbf{B}}{enB} \tag{18}$$

The terms participating in the parallel component of the electric field are a projection of the electric current on the magnetic field with the Coulomb conductivity, and the projection of the electron gas pressure gradient onto the magnetic field direction. The largest electric fields are generated at the foot-points of the current-carrying magnetic loops where the converging flows exists. Charge separation arises from the strongly magnetized electrons and weak ion magnetization. The electric field stipulated for the conductivity current $j_\parallel/\sigma$ on the right part of Eq. (18) is much less as a rule.

In a vertical axial-symmetric magnetic flux tube with convective plasma flow converging towards the tube axis, the gradient of electron gas pressure has radial direction and its value is (Zaitsev & Khodachenko 1997)

$$\frac{\partial p_e}{\partial r} = -\frac{1-F}{2-F}\frac{\sigma V_c B^2}{c^2(1+\alpha B^2)} \tag{19}$$

where $B^2 = B_\varphi^2 + B_z^2$, $\alpha = \sigma F^2/(2-F)c^2nm_i\nu_{ia}$, $\nu_{ia} \approx 6\times10^{-11}n_a\sqrt{T}$ (Golant et al. 1977). Hence

$$E_\parallel \approx \frac{1-F}{2-F}\frac{\sigma V_c B^2}{enc^2(1+\alpha B^2)}\frac{B_r}{B} \tag{20}$$

Here B_r is the radial component of the magnetic field in the flux tube. If no radial component of the tube magnetic field exists ($B_r = 0$) the large-scale electric field is perpendicular to the magnetic field ($E_\parallel = 0$) except for a small component $j_\parallel/\sigma$ which is unable to provide the required electron acceleration. Flute instability yields the penetration of plasma tongues into the current channel. As a result a radial component of the magnetic field appears and the electron acceleration in the quasi-static electric field of the magnetic flux tube becomes possible. From the induction equation (4) it follows that the acceleration process starts when the velocity of the penetrating plasma, V_0, depends on the altitude z, i.e., the plasma tongue should be restricted in altitude. Then from Eq. (4)

$$B_r(t) = B_z r\frac{\partial y(t)}{\partial z} \tag{21}$$

and for $\alpha B^2 \gg 1$

$$E_\parallel \approx \frac{1-F}{F^2}\frac{m_i\nu_{ia}V_c}{e}\frac{B_z}{B}r\frac{\partial y(t)}{\partial z} \tag{22}$$

The number of runaway electrons per second accelerated in DC-electric field is described by well-known formula (Knoepfel & Spong 1979)

$$\dot{N} = 0.35 n\nu_{ei}V\left(\frac{E_D}{E_\parallel}\right)^{3/8}\exp\left[-\sqrt{\frac{2E_D}{E_\parallel}}-\frac{E_D}{4E_\parallel}\right] \tag{23}$$

where V is the volume of the acceleration region, $E_D = m\nu_{ei}V_{T_e}/e$ is the Dreicer field, i.e., the field at which the critical velocity for electron acceleration out of thermal distribution equals the thermal velocity V_{T_e}. If for example the flute instability develops near the foot-point of the magnetic loop with the plasma parameters $n \approx 10^{11}$ cm^{-3}, $T \approx 10^5$ K, $r_0 \approx 10^8$ cm in the column of $h \approx 10^8$ cm, the observed values of $\dot{N} \approx 10^{35}$ el s^{-1} (Miller et al. 1997) reach at $E_D/E_\parallel \approx 25$. This gives $E_\parallel \approx 1.2\times10^{-3}$ V/cm, and the energy of accelerated electrons at the scale of $h \approx 10^8$ cm is about 120 keV. Hybrid thermal/nonthermal models require $\dot{N} \approx 10^{34}$ el s^{-1} (Holman & Benka 1992), and for the same plasma parameters we obtain $E_D/E_\parallel \approx 31$.

Therefore the intrusion of partially ionized plasma driven by flute instability into the current channel of a coronal magnetic loop simultaneously gives both the plasma heating and electron acceleration in the electric fields. For acceleration near the loop foot points these electric fields have sub-Dreicer values. In this case significant numbers of electrons are accelerated and even with sub-Dreicer electric fields no problem exists with the electron fluxes required for the hard X-ray emission observed. The productivity of the electron accelerator is thus in accord with observations. It is most important that the temporal dynamics of the plasma heating and electron acceleration depends on the time behaviour of the parameter $y(t)$. The physical sense of this parameter is the relative depth of the penetration of partially ionized plasma into the current channel of a loop. Eq. (16) determines various regimes of the energy release in a current-carrying magnetic loop.

Note, that Dennis et al. (1994) studied the evidence for both electron acceleration and plasma heating from DC-electric fields $(E_\parallel/E_D \sim 0.01)$ in solar flares. They did, however, not address the origin of the electric field.

4. Pulsating and explosive regimes

The time profiles of the mm-wave emission presented in Sect. 2 reflect temporal evolution of plasma heating and particle acceleration at a flare site because the radio emission at mm-wavelengths is most probably due to bremsstrahlung and/or gyrosynchrotron processes. Deviations of plasma pressure in a magnetic loop and particle acceleration rate are determined, in turn, by $y(t)$ given in Eq. (16). We will show that different regimes of the energy release can be realized in a single current loop depending on the values of the parameter $\varepsilon = t_c/t_A$ which characterizes the rate of energy release, parameter ε_1 which determines the damping of MHD-oscillations, and the initial conditions.

Eq. (16) describes the pulsating and explosive energy release, but in general case the solution can be obtain only numerically. Here we consider analytically the particular case $\varepsilon \ll 1$, $\varepsilon_1 \ll 1$. This case can be realized in the dense chromospheric layers where the time scale of Joule heating driven by ion-atom collisions t_c is much less than the Alfvénic transit time t_A. So, we can omit the term $2\varepsilon\varepsilon_1 y\partial y/\partial t$ in Eq. (16) and find the solution in the form

$$y(\tau) = A(\tau)\sin\tau + y_0(\tau) \tag{24}$$

The unknown functions $A(\tau)$ and $y(\tau)$ describe the slow variation of the pulse amplitude in time and gas pressure gradient averaged over the pulsation period. Substituting Eq. (24) into the non-linear equation (16) and of the averaging over the fast time we find the following set of non-linear equations for both $A(\tau)$ and $y_0(\tau)$:

$$\frac{dA}{d\tau} = -A(\varepsilon y_0 + \frac{\varepsilon_1}{2}) \tag{25}$$

$$\frac{dy_0}{d\tau} = \varepsilon(\frac{A^2}{2} + y_0^2) \tag{26}$$

The pulsation magnitude $A(\tau)$ and the function of $y_0(\tau)$ vary slowly, with typical time scale $\sim 1/\varepsilon$. $y_0(\tau)$ determines the dimensionless function p_0 (see Eq. (9)) averaged over the pulsation period:

$$y_0 = \frac{1}{2\pi}\int\limits_{\tau}^{\tau+2\pi}\frac{p_0(\tau')}{(B_0^2/2\pi)}d\tau' \tag{27}$$

It is quite easy to convince ourself of this fact when substituting Eq. (24) into Eq. (14) and averaging.

An important peculiarity of Eq. (26) is that the derivative $dy_0/d\tau$ is always positive. It means that at $r < r_0$ the gas pressure in the periphery of flux tube grows faster than near the axis. This effect is due to the *r*-dependence of the Ampère force and Joule heating (see Eqs. (7) and (14)). The gas pressure gradient becomes positive and high until it starts accelerating the plasma tongue penetrating into the current channel due to the flute instability. We will show that this process is responsible for the explosive energy release.

Let us consider the special case when the velocity of the tongue is small, $V_0^2 \ll V_{T_i}^2\beta$, where $\beta = 8\pi p_0/B_0^2$. In this case $A^2/2 \ll y_0^2$, and from Eqs. (25) and (26) we obtain

$$y_0(\tau) = A(0)[1 - y_0(0)\varepsilon\tau]e^{-\frac{\varepsilon_1}{2}\tau}\sin\tau + \frac{y_0(0)}{1-y_0(0)\varepsilon\tau} \tag{28}$$

Physically the energy release can be divided into two classes.

(i) When the initial gas pressure in the loop decreases to the periphery but is high enough, $y_0(0) < -\varepsilon_1/2\varepsilon$, the pulsation amplitude first grows with typical time scale $\tau \sim 1/\varepsilon|y_0(0)|$ and then decreases for the time $t_d \approx r_0/V_A\varepsilon_1$. This case corresponds to the time profiles of the mm-wave emission in Fig. 2a. For $-\varepsilon_1/2\varepsilon < y_0(0) < 0$ the solution of Eq. (28) gives pulsations with slowly damped magnitudes as in Fig. 2b. Both cases

can be realized in a flare loop when the gas pressure inside the flux tube is high, $\beta(0) \sim 1$.

(ii) In the opposite case when the gas pressure increases from the tube axis towards periphery, $y_0(0) > 0$, the gas pressure and flux of accelerated particles increase explosively. This is described by the last term on the right of Eq. (28). The characteristic time of the explosive process is

$$t_E \approx \frac{1}{y_0(0)\varepsilon}\frac{r_0}{2V_A} \tag{29}$$

When the damping time $t_d \approx r_0/V_A\varepsilon_1$ is less compared with the explosive phase as given by (29), $y_0(0) < \varepsilon_1/2\varepsilon = 3/8$ (low pressure plasma), the pulsations occur before the explosive phase (Fig. 4a). For high pressure in the loop, $y_0(0) \geq \varepsilon_1/2\varepsilon$, pulsations either superimpose upon the explosive time profile (Fig. 4c) or follow the explosive phase (Fig. 4b).

5. Discussion and concluding remarks

The Metsähovi data at 22 and 37 GHz the flares have very different time histories. *(i)* Pulsations with large amplitudes (Fig. 2a,b). *(ii)* Single pulse with fast increase and relative slow decay Fig. 3). *(iii)* Pulsations superimposed upon bulk burst (Fig. 4a,c), and pulsations followed by explosive phase (Fig. 4b). These examples show that the temporal dynamics of flare energy release should contain pulsating and explosive regimes. The two-colliding- loop model (Tajima et al. 1987) explains to some extent the time profile of the types *(i)* and *(iii)* bursts similar to the event in Fig. 2b, and 4a,b, but do not explain the time profile of type *(ii)*. Moreover the model of Tajima et al. (1987) holds in the special case of two identical current loops. It is not clear, however, what happens in the more realistic case of non-symmetric loops. From the other side, recent Yohkoh and Nobeyama observations provide strong evidence that flares often occur in a simple loop configuration.

Attempts to explain the pulsation structure of the flare emission were made by several authors (see review of Aschwanden 1987). In order to search the periodic modulation of the loop magnetic field, a MHD-approach was commonly used. Then the effect of field oscillations on the time behaviour of flare emission in different wave bands was took into account. This approach is non-self-consistent because the reaction of magnetic field variation on the rate of energy release is ignored. Thus, in the frame of that approach it is impossible to get an explosive energy release or the combination of pulsating and explosive regimes.

In this paper, we took into account the response of the energy release rate in a loop to magnetic field variations driven by a tongue of surrounding plasma. As flare trigger we considered the flute instability producing the intrusion of cold partially ionized plasma of the prominence (near the loop top) or chromosphere plasma (near the loop foot points) into the current channel of a loop. In this case the energy release is accompanied by plasma heating due to Joule dissipation of electric current driven by ion-atom collisions under non-steady-state regime of plasma injection into a magnetic loop, and by electron acceleration in DC-electric field. The current dissipation required for a flare is provided by the increase of the loop plasma resistance and is 7–9 orders higher than in the pre-flare stage.

In present paper, we took into consideration the response of the Ampère force arising from the deformation of initially force-free magnetic flux tube by the plasma intrusion into the current channel. This self-consistent approach helps us to understand why flare energy release driven by flute instability occurs in initially force-free flux tubes with $\beta \ll 1$. A plasma tongue entering into a force-free current channel ($\mathbf{j} \parallel \mathbf{B}$) deforms the tube magnetic field and causes a Ampère force (Eq. (7)). This force prevents the penetration of a tongue, and its magnitude grows from the tube axis towards the periphery up to the surface at $r = r_0$. The plasma is heated faster near the channel surface than in the tube axis (see Eqs. (3)and (7)). This heating becomes more effective due to the repeated (oscillating) penetration of a plasma tongue into the current channel. The gradient of gas pressure directed towards the flux tube surface compensates the Ampère force completely and causes an explosive energy release. Wheatland & Melrose (1995) omitted the effect of inhomogeneous heating of the current channel in their analysis of energy release in a force-free current-carrying loop and obtained a resistance four orders less than required for a flare. Our self-consistent model yields a powerful energy release in initially force-free magnetic loop.

The Joule heating rate per unit volume is given by Eq. (14). Let us estimate the total heating rate in the case when a flare develops near the foot-points of a loop with radius $r_0 \approx 10^8$ cm in the column of $h \approx 10^8$ cm. The energy release volume is about 3×10^{24} cm^3. From Eq. (12) for a typical plasma tongue velocity $V_0 \approx V_{T_i} = 3 \times 10^6$ cm s^{-1} and burst duration $\triangle t \approx 10$ s we obtain a maximum value of $y \approx 0.3$. Supposing that at the loop foot-points $n \approx 10^{11}$ cm^{-3} and $T \approx 10^5$ K we find the Joule heating rate: $Q \approx 6 \times 10^{27}(B_0/10^3)^4 F$ erg s^{-1}. The heating rate depends strongly on the loop magnetic field and on the relative density of neutrals, F. In order to explain the hard X-ray emission, the accelerator has to supply $\dot{N} \approx 10^{35}$ el s^{-1} (Miller et al. 1977). From Eq. (23) we obtain $E_D/E_\parallel \leq 25$, and using Eq. (22) we find $F \leq 0.15$. Here we suppose $\triangle z \sim r_0$ i.e. $B_r/B \sim y \sim 0.3$.

Now we can compare the heating rate Q and acceleration rate Q_a in our single-loop flare model. For medium energy electrons (20 keV) Eq. (23) gives $Q_a \sim 3 \times 10^{27}$ erg s^{-1}, and $Q/Q_a \sim 2F(B_0/10^3)^4$. Depending on the magnetic field value in the loop, Joule heating can be either more or less effective then electron acceleration. For $B_0 > 1300$ G the heating prevails over acceleration. In comparatively week magnetic fields particle acceleration is more effective. Observations of solar flares provide evidence that the ratio Q/Q_a varies from event to event (Wu et al. 1986). Note that the strong dependence of the Joule heating on the magnetic field was to be expected from Eq. (3): $Q \propto (\mathbf{j} \times \mathbf{B})^2 \propto B^4$. The Joule heating rate obtained by Holman, Kundu & Kane (1989) gives $Q \propto B$.

We have shown that the gas pressure-gradient is very important in the flare model and is essential for the temporal behavior

of the energy release. The following modes of energy release are possible in the frame of our self-consistent approach.

1. If the initial gradient of the gas pressure in a loop is negative, $y_0(0) < 0$, e.g. gas pressure drops from the loop axis, a pulsating energy release occurs with typical period $P \approx \pi r_0/V_A$ which is of the order of the Alfvén transit time. This case fits well for the explanation of the time profiles consisting of the pulses with deep modulation (type *'i'* in our classification) or single pulse (type *'ii'*). Single pulse occurs when pulsation period is of order of damping time of pulsations $t_d \approx r_0/V_A\varepsilon_1$.
2. When the initial gradient of the gas pressure is positive, $y_0(0) > 0$, e.g. the gas pressure grows towards the periphery of the tube, flute instability leads to co-existing pulsating and explosive regimes. The lifetime of the pulsation phase $t_d \approx r_0/V_A\varepsilon_1$ can be shorter or longer than the time scale of the explosive phase $t_E = r_0/y_0(0)\varepsilon V_A$. In the first case ($t_d < t_E$) pulsations appear before the explosive phase (Fig. 4a). In the second case pulsations are either superimposed upon the explosive burst (Fig. 4c) or followed by the explosive phase (Fig. 4b).

We have not considered the energy losses (electron heat conductivity, viscosity, radiation losses etc.) from the energy release volume. It should be noted also that the additional saturation and switch-off of the energy release may be connected with an increasing ionization rate in the flare process, which gives a decreasing ratio of Joule heating driven by ion-atom collisions. The electron heat conductivity and radiation losses have been accounted for in the numerical analysis. We found that both factors do not introduce any noticeable changes of the conclusions concerning the pulsating and explosive energy release.

During the pulsating and explosive regimes of Joule heating of the flare plasma, electron acceleration by DC-electric field operates simultaneously and with the same time history. This is in favor of the paradigm that heating and acceleration are two aspects of the flare process (Güdel & Benz 1993; Linsky 1996). This circumstance explains also the in-phase time profiles of microwave and hard X-ray emission of solar flares (Lee & Wang 1998). Finally, we have to note that our interpretation of mm-wave emission of solar flares under various dynamical regimes should be considered as tentative because we can not determine the emission mechanism (bremsstrahlung or gyrosynchrotron) nor the optical depth of a source in each case. Depending on the radio emission mechanism and on the optical thickness of the source the observed flux of mm-wave emission reflects both the plasma heating and particle acceleration processes in the flare region in different ways.

Acknowledgements. This work was supported by INTAS-RFBR grant 95-316, RFBR grants 99-02-16045 and 00-02-16356, and by the Academy of Finland. The authors thank Dr. M.Khodachenko for the numerical analysis of the problem.

References

Alfvén H., Carlqvist P., 1967, Solar Phys. 1, 220
Aschwanden M.J., 1987, Solar Phys. 111, 113
Benz A.O., Barrow C.W., Dennis B.R., et al., 1983, Solar Phys. 83, 267
Bray R.J., Loughhead R.E., Durrant C.J., 1984, The Solar Granulation, Cambridge Univ. Press
Cargill P.J., Chen J., Garren D.A., 1994, ApJ 423, 854
Chargeishvili B., Zhao J., Sakai J.I., 1993, Solar Phys. 145, 297
Chiuderi Drago F., Alissandralis C., Bentley R.D., Philips A.T., 1998, Solar Phys. 182, 459
Colgate S.A., 1978, ApJ 221, 1068
Cowling T.G., 1957, Magnetogydrodynamics, Intersci. Publ. Inc. NY
Dennis B.R., Holman G.D., Hudson H.S., et al., 1994, Proc. Kofu Symp. NRO Rep. # 360, 217
Doshek G.A., Strong K.T., Tsuneta S., 1995, ApJ 440, 370
Enome S., 1996, In: Uchida Yu. et al. (eds.) Magnetodynamic Phenomena in the Solar Atmosphere, Kluwer, p. 195
Golant V.E., Zhilinsky A.P., Sakharov I.E., 1977 Basis of Plasma Physics, Atomizdat, Moscow
Güdel M., Benz A.O., 1993, ApJ Lett. 405, L63
Henoux J.C., Somov B.V., 1991, A&A 241, 613
Heyvaerts J., Priest E.R., Rust D.M., 1977, ApJ 216, 123
Holman G.D., 1985, ApJ 293, 584
Holman G.D., Kundu M.R., Kane S.R., 1989, ApJ 345, 1050
Holman G.D., Benka S.G., 1992, ApJ Lett. 400, L79
Kan J.R., Akasofu S.-I., Lee L.C., 1983, Solar Phys. 84, 153
Kane S.R., Kai K., Kosugi T., et al., McKenzie D.L., 1983, ApJ 271, 376
Knoepfel H., Spong D.A., 1979, Nucl. Fusion 19, 785
Kucera T.A., Love P.J., Dennis B.R., et al., 1996, ApJ 466, 1067
Lee C.-Y., Wang H., 1998, BBSO Preprint, # 1032
Linsky J.L., 1996, ASP Conf. Ser. 93, 439
Marsh K.A., Hurford G.J., 1980, ApJ Lett. 240, L111
Masuda S., 1994, Hard X-ray Sources and the Primary Energy Release Site in Solar Flares, Dissertation, Yohkoh HXT group, NAO, Mitaka, Tokyo
Mikhailovskii A.B., 1975, Theory of Plasma Instabilities, Vol. 2, Consultans Bureau, NY
Miller J.A., Cargill P.J., Emslie A.G., et al., 1977, JGR 102, 14631
Nakajima H., Kosugi T., Kai K., et al., 1983, Nature 305, 292
Nishikawa K., Sakai J., Zhao J., et al., 1994, Proc. Kofu Symp. NRO Rep. # 360, 255
Priest E.R., 1982, Solar Magnetohydrodynamics, Reidel, Dordrecht
Priest E.R., 1985, In: Priest E.R.(ed.) Solar Flare Magnetohydrodynamics, Gordon & Breach
Pustil'nik L.A., 1973, AZh 50, 1211
Roberts B., Edwin P.M., Benz A.O., 1984, ApJ 297, 857
Rosenberg H., 1970, A&A 9, 159
Sakai J.-I., de Jager C., 1996, Space Sci. Rev. 77, 1
Sakai J.-I., de Jager C., 1997, Solar Phys. 173, 347
Sakao T., Kosugi T., 1996, In: Uchida Yu., et al.(eds.) Magnetodynamic Phenomena in the Solar Atmosphere, Kluwer, 169
Sato J., Sawa M., Masuda S., et al., 1998, The Yohkoh HXT Image Catalogue, Oct. 1991 - Aug. 1998, NRO/NAO
Schrijver C.J., Title A.M., Berger T.E., et al., 1999, Solar Phys. 187, 261
Sen H.K., White M.L., 1972, Solar Phys. 23, 146
Spicer D.F., 1977, Solar Phys. 53, 305
Stepanov A.V., Urpo S., Zaitsev V.V., 1992, Solar Phys. 140, 139
Tajima T., Sakai J., Nakajima H., et al., 1987, ApJ 321, 1031

Tsuneta S., 1985, ApJ 290, 353
Tsuneta S., 1996, ApJ 456, 840
Tsuneta S., Hara H., Shimizu T., et al., 1992, PASJ 44, L63
Uchida Yu., Shibata K., 1988, Solar Phys. 116, 291
Urpo S., Pohjolainen S., Terasranta H., 1992, Solar Radio Flares 1989–1991, HUT Report 11, Ser. A
Wheatland M.S., Melrose D.B., 1995, Solar Phys. 159, 137
Wu S.T., de Jager C., Dennis B.R., et al. 1986, Flare Energetic, In: Energetic Phenomena on the Sun, NASA C P 2439, Part 5
Zaitsev V.V., Khodachenko M.L., 1997, Radiophysics & Quantum Electronics 40, 114
Zaitsev V.V., Stepanov A.V., 1992, Solar Phys. 139, 343
Zaitsev V.V., Stepanov A.V., Urpo S., Pohjolainen S., 1998, A&A 337, 887